Journal of Flow Visualization & Image Processing, vol. 3, pp. 265–277, 1996

CORRECTION OF PIV IMAGE BIASING USING TWO CO-ROTATING MIRRORS

K. D. Kihm
Department of Mechanical Engineering, Texas A&M Universtiy, College Station, TX 77843–3123
S. D. Lee and S. H. Chung
Department of Mechanical Engineering, Seoul National University, Seoul 151–742, Korea

The rotating mirror configuration in particle image velocimetry (PIV) is generally used to provide an artificial image shift to resolve the directional ambiguities for the recorded particle image pairs. However, the reflected image from the rotating mirror inevitably creates normal velocity components with respect to the image plane, and this normal component causes spatially distributed systematic image errors. A potential solution for the problem is proposed to replace the single rotating mirror with two co-rotating mirrors. The use of two co-rotating mirrors reduces the image biasing with desired amounts of the velocity shift available, and, at the same time, makes the image biasing uniform on the entire image field so that analytical corrections for the biasing are readily feasible. Detailed imaging kinematics of the suggested method are presented to improve the design of practical PIV systems. Also presented is experimental confirmation of the image correction using two co-rotating mirrors.

INTRODUCTION

The most widely used method for resolving the directional ambiguities in PIV is to artificially generate a velocity shift of the second recorded image using a rotating mirror [1]. The shift velocity is added to the flow field so that all the apparent particle displacements are consistent in their sign. Subtracting the shift velocity from the measured particle image velocity determines the real (positive or negative) flow velocity.

When the PIV mirror rotates, the reflected image also rotates, tilts, and shifts simultaneously between the two exposures. The image tilting generates a spatially distributed normal velocity component with respect to the focal plane of the recording system. This induced normal velocity component tilts the perspective view of the particle images, and the recorded particle displacement is biased either shorter or longer than it should be. Therefore, the velocity measurement analysis from the particle displacement recorded with a rotating mirror PIV system is subjected to systematic errors [2].

Raffel and Kompenhans [3] suggested a computational technique to correct the systematic errors as a post-data correction of images taken by a rotating mirror PIV system. They demonstrated a successful application of the PIV system with an enhanced accuracy in detecting particle image displacement. Although the computational correction technique could eliminate the systematic image errors effectively, the image blur problem intrinsically occurring from the normal displacement of the rotating images is not yet resolved.

The proposed correctional method uses two co-rotating mirrors instead of a single rotating mirror in order to reduce the systematic errors and image blurs. The key idea is to devise a velocity shifting configuration that minimizes the normal velocity component with respect to the focal plane of the recording system. First, the generalized image kinematics reflected from moving/rotating mirrors is briefly outlined and the image biasing generated by a rotating mirror method is identified for a nonzero normal velocity component. The suggested method using two co-rotating mirrors will then be discussed using the comprehensive image kinematics. A simulated PIV experiment using synthesized dot images will also be discussed to confirm the theoretical findings.

KINEMATICS OF MIRROR IMAGES

A general expression for the reflected image velocity is derived from the basic principle of mirror image kinematics. Geometrical considerations of mirror reflection of an arbitrary vector $\vec{r}$ to a virtual object vector $\vec{r}'$ give a simple mathematical expression as (Fig. 1a):

$$\vec{r}' = \vec{r} - 2(\vec{r} \cdot \vec{n})\vec{n} = (\delta_{ij} - 2n_i n_j)\, r_j = R_{ij} r_j = [R] \cdot \vec{r} \tag{1}$$

where

$$[R] \equiv R_{ij} \equiv \delta_{ij} - 2n_i n_j \tag{1a}$$

conforms to a reflection matrix and $\vec{n}$ denotes a unit vector defined normally outward from the mirror surface. When a mirror rotates around the z-axis, that is, plane rotation with a single degree of freedom, the unit normal vector is given as

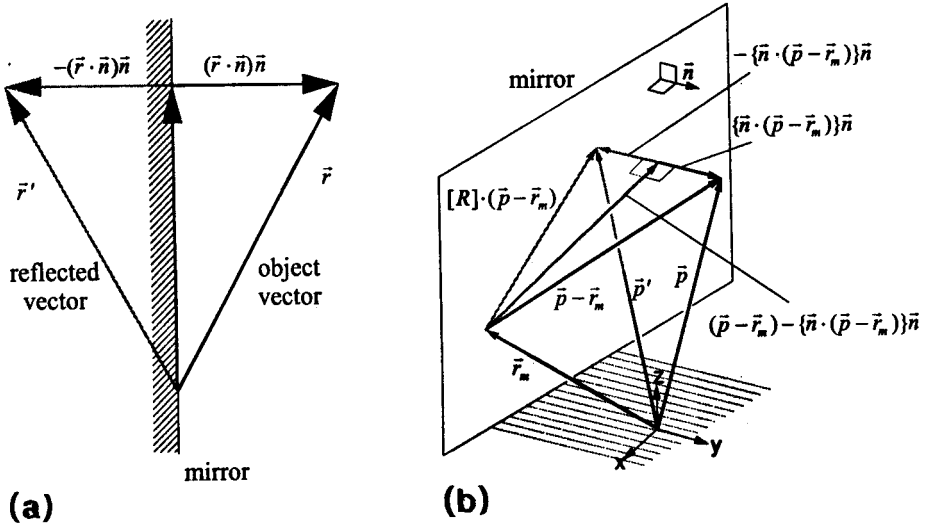

Fig. 1 Illustration of mirror image reflections.

$$\vec{n} = (\sin\theta, -\cos\theta, 0) \tag{1b}$$

where the mirror angle θ is measured from the x-axis.

From Eqs. (1a) and (1b), the reflection matrix $[R]$ is expressed as

$$[R] = \begin{bmatrix} \cos 2\theta & -\sin 2\theta & 0 \\ \sin 2\theta & \cos 2\theta & 0 \\ 0 & 0 & 1 \end{bmatrix} \begin{bmatrix} 1 & 0 & 0 \\ 0 & -1 & 0 \\ 0 & 0 & 1 \end{bmatrix} \tag{2a}$$

and its time derivative is given as

$$\frac{d[R]}{dt} = 2\omega \begin{bmatrix} \cos(2\theta + 90°) & \sin(2\theta + 90°) & 0 \\ \sin(2\theta + 90°) & -\cos(2\theta + 90°) & 0 \\ 0 & 0 & 0 \end{bmatrix} \tag{2b}$$

Equation (2a) interprets the reflection matrix to form two elementary movements represented by the two matrices: a mirror imaging with respect to the x-axis and a rotation by an angle 2θ.

The above basic image kinematics are extended to derive a general expression for the reflected image velocity. When an arbitrary position vector $\vec{r}_m$ specifies the mirror location (Fig. 1b), the image vector $\vec{p}'$ is equivalent to the reflection of an arbitrary position vector $\vec{p}$ and Eq. (1) gives:

$$\vec{p}' = [R] \cdot (\vec{p} - \vec{r}_m) + \vec{r}_m \tag{3}$$

A time derivative of the reflected vector $\vec{p}'$ determines the velocity of the reflected image, i.e.,

$$\vec{v}_{image} = \frac{d\vec{p}'}{dt} = \frac{d}{dt}\{[R] \cdot (\vec{p} - \vec{r}_m) + \vec{r}_m\} \tag{4}$$

Expanding the derivative, applying vector identities, and using useful vector relationships of $d\vec{n} / dt = \vec{\omega} \times \vec{n}$ and $\vec{\omega} = \vec{n} \times d\vec{n} / dt$ (see Appendix A), Eq. (4) derives a general three-dimensional expression for the reflected image velocity as:

$$\vec{v}_{image} = 2\vec{\omega} \times \{[R] \cdot (\vec{p} - \vec{r}_m)\} + 2(\vec{v}_m \cdot \vec{n})\vec{n} + [R] \cdot \vec{v} \tag{5}$$

where $\vec{\omega}$ is the angular velocity of a rotating mirror, $\vec{v}_m$ denotes the traversing velocity of the mirror defined as $\vec{v}_m \equiv d\vec{r}_m / dt$, and $\vec{v}$ represents the object velocity defined as $\vec{v} \equiv d\vec{p} / dt$. Note that the mirror rotation vector $\vec{\omega}$ has only the z-directional component

for the plain mirror rotation. The first term on the RHS, due to the vector product by $\vec{\omega}$, will not carry any z-directional component.

This first term on the RHS of Eq. (5) represents the portion of the image velocity created by the plain mirror rotation that exists only in the x-y plane. The second term is a contribution from the mirror traversing perpendicular to the mirror surface. When the mirror traversing takes place in the plane perpendicular to the mirror surface, this term also retains its component within the x-y plane. The third term reflects the mirror imaging of the real velocity of a moving object, $\vec{v}$. The object velocity can be arbitrarily three-dimensional. In fact, the general expression for the image velocity $\vec{v}_{image}$ in Eq. (5) can be three-dimensional only if the third term, the object velocity, is three-dimensional.

Note also in Eq. (5) that the only possible time-dependent property is the particle position vector $\vec{p}$ that changes with the particle movement. Thus, only the first term can be subjected as time-dependent. The second and third terms remain time invariant when the mirror traverses at a constant velocity $\vec{v}_m$, and the particle velocity remains steady at $\vec{v}$ during the PIV sample period. However, as shown in the next section for a two co-rotating mirror system, the recorded PIV image velocity $\vec{v}_{image}$ is invariant with respect to time when the mirrors are rotating with a single degree of freedom, that is, around one rotating axis z.

SYSTEMATIC PIV IMAGE BIASING GENERATED BY A SINGLE ROTATING MIRROR

Figure 2 shows the image plane reflected by a rotating mirror at an angular velocity $\vec{\omega}$. This is a simple or plain rotating case reduced from the arbitrarily moving mirror system shown in Fig. 1b. The coordinate is set to originate from the center of view on the image plane and the y- or n-coordinate is set perpendicular to the plane. The image of a stationary object ($\vec{v} = 0$) is assumed at (x, z) on the image plane. The second term in Eq. (5) then vanishes because there is no traversing motion of the mirror, and the third term also vanishes for the stationary object under consideration. Because $\vec{\omega} = (0,0,\omega)$ and $[R] \cdot (\vec{p} - \vec{r}_m) = (x, -L_2, z)$, Eq. (5) reduces to

$$\vec{v}_{image} = (2\omega L_2, 2\omega x, 0) \tag{6}$$

The spatially uniform tangential- or x-component $v_t = 2\omega L_2$ provides the image shifting to resolve the directional ambiguities in PIV, and the normal velocity component $v_n = 2\omega x$ enlarges (when positive or approaching) or reduces (when negative or escaping) the perspective view size, which attributes to the image biasing. Thus, the tangential projection of the normal velocity component dictates the magnitude of the image biasing, and for the counterclockwise rotation shown in Fig. 2, the tangential projection $\hat{v}_n$ is given from the trigonometry:

$$\hat{v}_n(x, z) = v_n \tan\alpha = 2\omega x \frac{l}{L_1} = \frac{2\omega}{L_1} x\sqrt{x^2 + z^2} \tag{7}$$

where α denotes the perspective viewing angle. The normal velocity directing away from the reflected image in the negative x reduces the perspective view, and the normal velocity

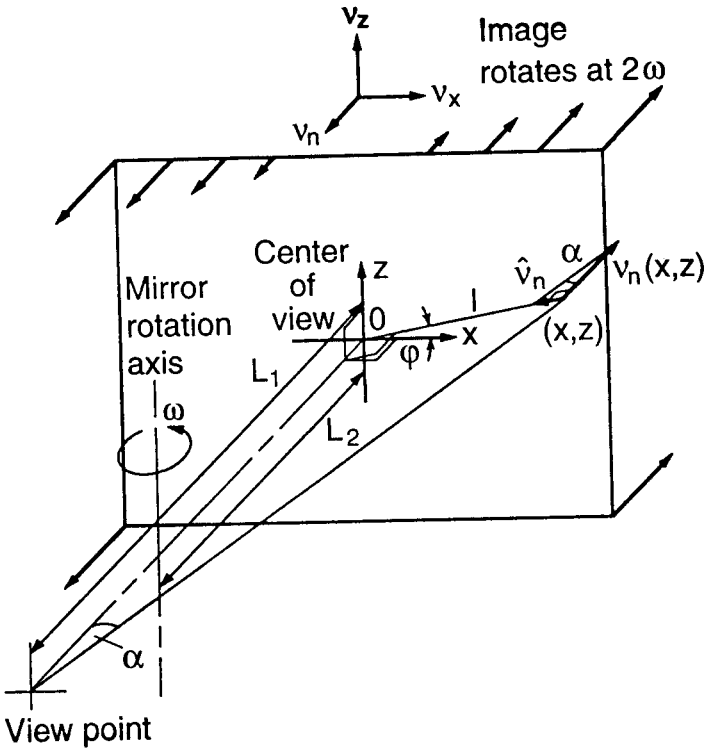

Fig. 2 Illustration of a normal velocity component on the image plane caused by a rotating mirror.

approaching the image plane in the positive x enlarges the perspective view. Note that the tangential projection of the normal image velocity described by Eq. (7) is spatially distributed on the x-z image plane, but independent of the mirror position angle θ. This means that the amount of image biasing at a fixed location (x, z) remains fixed during the entire rotation of the mirror. This feature enables the numerical corrections of the image biasing occurring from a single-mirrored PIV system.

Figure 3 shows the spatially dependent image biasing per unit time, $\bar{v}_{bias}(x, y)$, which is derived from Eq. (7) as

$$\bar{v}_{bias}(x, z) = \frac{2\omega}{L_1}(x^2, xz) \tag{8}$$

The arrow length represents the magnitude of image biasing. The radially inward arrows denote a reduction in the recorded image size, and the radially outward arrows represent an enlargement of the recorded image size. The arrow direction is reversed symmetrically with respect to the z-axis. The magnitudes of the normal displacements are symmetrically distributed along the x-axis. The amount of the actual image biasing in the PIV recording is determined from Eq. (8) multiplied by the PIV sample period required for the double recordings. The optimal PIV recording period is determined from a combinatorial consideration of the flow speed and the particle image sizes.

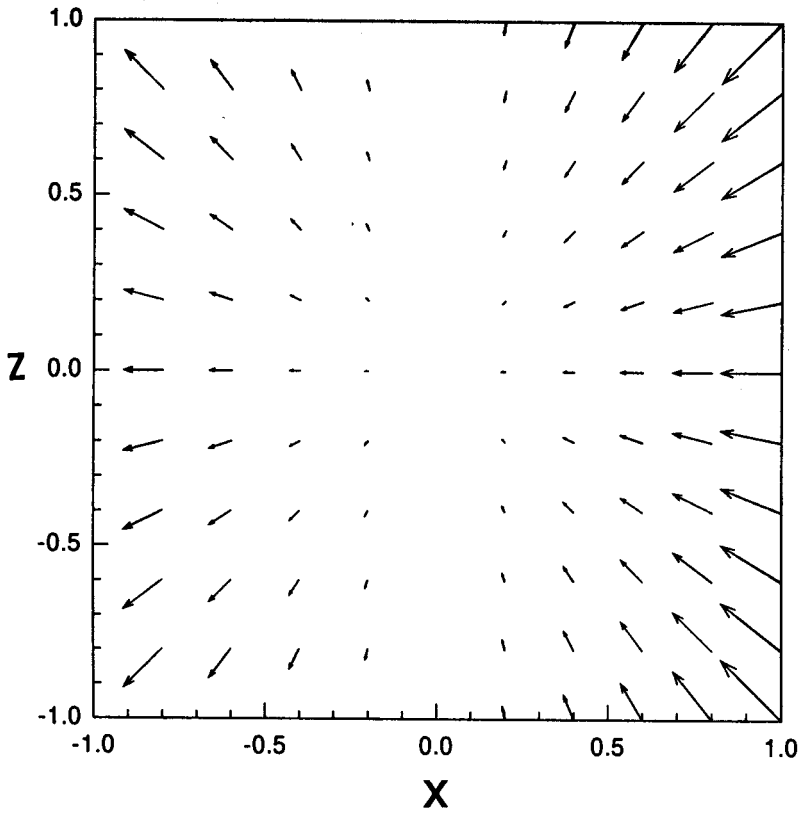

Fig. 3 Two-dimensionally distributing systematic PIV image biasing occurring from a singler-rotating mirror system (Eq. [8]).

DOUBLE REFLECTION BY TWO CO-ROTATING MIRROR SYSTEM

It is shown that a single rotating mirror inevitably creates the two-dimensionally varying normal displacement because of nonzero normal velocity component. This nonzero normal displacement, or normal velocity component, causes the systematic errors of the recorded PIV images. Instead of one mirror, the use of two parallel and co-rotating mirrors at the same angular speed can reduce image biasing. The first reflected image of a stationary object in Fig. 4 rotates counterclockwise at an angular speed of 2 ω around the first mirror axis. Because the first mirror counterrotates against the image of the first mirror (reflected by the second mirror), the second reflected image has only revolutionary (self-rotating) displacement with no image tilting.

A mathematical description of the co-rotating two-mirror system follows. The general expression for the reflected image velocity, Eq. (5), reduces to a simpler form for a rotating but nontraversing first mirror ($\vec{v}_{m_1} \equiv 0$) with a stationary object ($\vec{v} \equiv 0$):

$$\vec{v}_{image_1} = 2\vec{\omega} \times \{[R] \cdot (\vec{p} - r_{m_1})\} \tag{9}$$

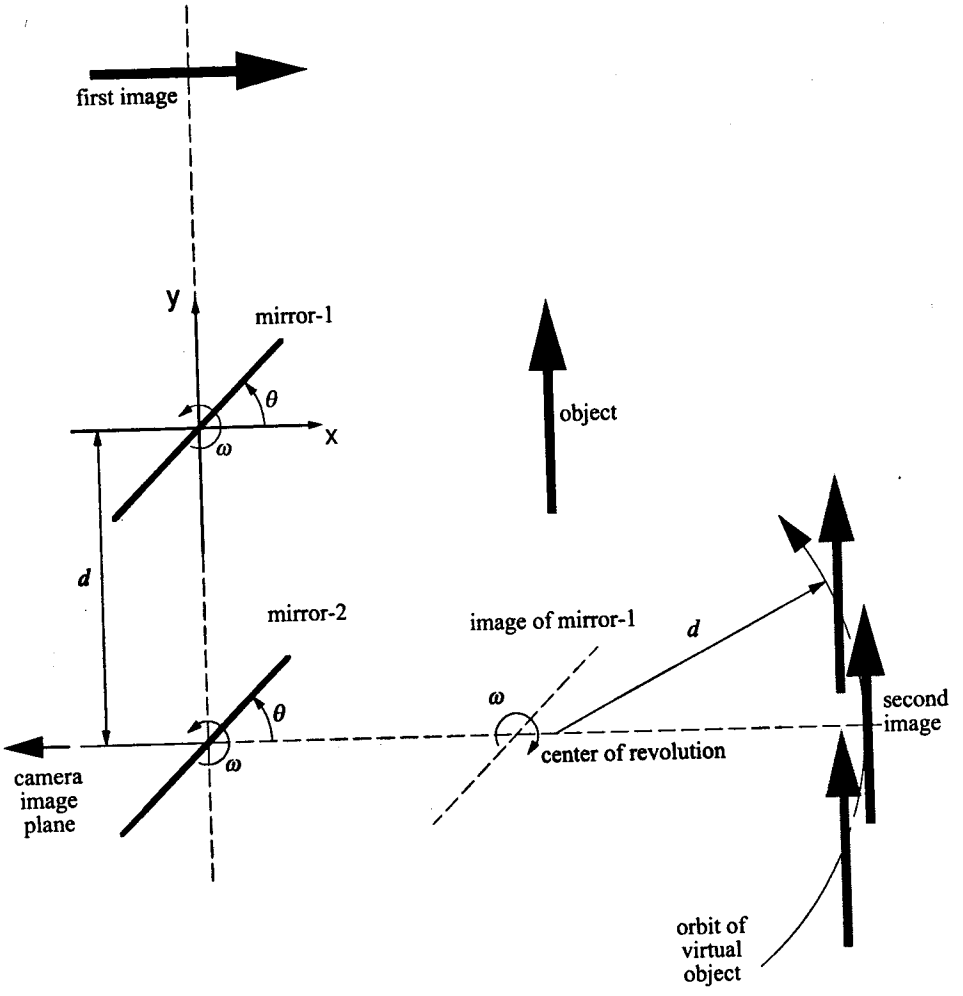

Fig. 4 Schematic of double reflections of an object by two parallel and co-rotating mirrors.

where $\vec{r}_{m_1}$ denotes the position vector (Fig. 1b) of the rotational axis of the mirror-1 (Fig. 4). When the z axis is set to coincide with the mirror-1 axis, the mirror position vector $\vec{r}_{m_1}$ is zero. The mirror rotation vector $\vec{\omega} = (0,0,\omega)$, and the arbitrary position vector $\vec{p} = (x, y, z)$ (Fig. 1b). The velocity of the first reflected image is then given as

$$\vec{v}_{image_1} = 2\omega \begin{bmatrix} 0 & -1 & 0 \\ 1 & 0 & 0 \\ 0 & 0 & 0 \end{bmatrix} \cdot \left(\begin{bmatrix} \cos 2\theta & \sin 2\theta & 0 \\ \sin 2\theta & -\cos 2\theta & 0 \\ 0 & 0 & 1 \end{bmatrix} \cdot \begin{pmatrix} x \\ y \\ z \end{pmatrix} \right) \tag{10}$$

where θ denotes the mirror slope angle measured with respect to the x-axis as shown in Fig. 1 or Fig. 4.

The second mirror position vector $\vec{r}_{m_2} = (0, -d, 0)$ where d is the distance between the first and second mirror axes. The second image sees the first image as a virtual object, which traverses at $\vec{v}_{image_1}$, and Eq. (5) for the second reflected image is expressed as

$$\begin{aligned}\vec{v}_{image_2} &= \vec{\omega} \times \{[R] \cdot (\vec{p}_{image_1} - \vec{r}_{m_2})\} + [R] \cdot \vec{v}_{image_1} \\ &= 2\vec{\omega} \times ([R]: [R] \cdot \vec{p}) - 2\vec{\omega} \times \left([R] \cdot \vec{r}_{m_2}\right) + [R] \cdot \vec{v}_{image_1} \end{aligned} \tag{11}$$

Substituting Eq. (10) into Eq. (11) gives a strikingly simple expression for the second reflected image velocity:

$$\vec{v}_{image_2} = 2\omega d\,(\cos 2\theta, \sin 2\theta, 0) \tag{12}$$

The y-component of $\vec{v}_{image_2}$ provides a tangentially shifted velocity to alleviate the directional ambiguities. The x-component represents the normal velocity component whose projection onto the image plane conforms to the image biasing (Fig. 2). Note that the PIV image velocity, Eq. (12), is time-independent despite the mirror rotations. The time dependence, or equivalently, the position vector variation of the recorded object, $\vec{p} = (x, y, z)$ appearing in the first term of Eq. (11) disappears because of the compensation from the third term of the same equation.

Figure 5 shows the normal velocity component and the velocity shift normalized by $2\,\omega d$ as functions of θ. It is emphasized that the co-rotating two-mirror system generates a spatially uniform normal velocity component, the x-component of Eq. (12), in the entire

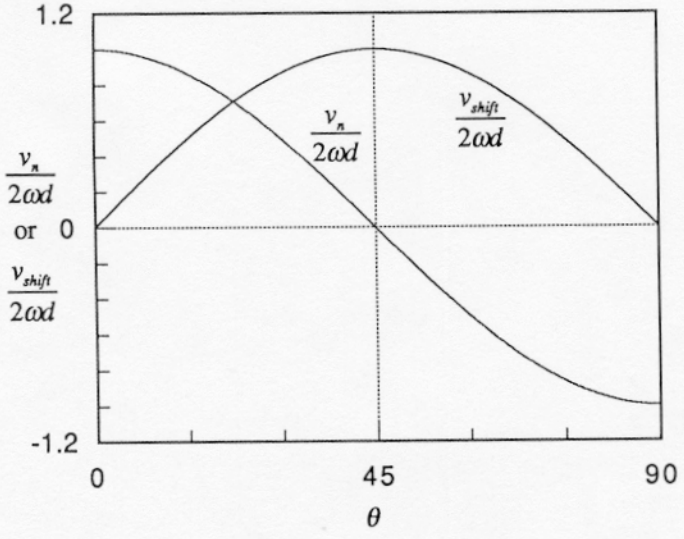

Fig. 5 Normal and tangential velocity components of the image taken by the two co-rotating mirror system vs. the mirror slope angle at which the image is recorded.

image field recorded at a given θ. In summary, the normal component of the image velocity, Eq. (6) or (12), is given as:

$$v_n = 2\omega x \qquad \text{PIV with a single rotating mirror} \tag{13a}$$

$$v_n = 2\omega d \cos 2\theta \qquad \text{PIV with two co-rotating mirrors} \tag{13b}$$

whose projections onto the image plane give the image biasings, respectively (Fig. 2). The projection of Eq. (13a) generates the two-dimensionally varying image biasing shown in Eq. (8) for the single rotating mirror case. For the case of two co-rotating mirror PIV, the image biasing will be uniform because Eq. (13b) is constant. Also, zero image biasing is expected when both PIV images are taken at $\theta = 45°$. This situation of zero image biasing, however, does not allow transit time recordings that are necessary for PIV measurement.

The tangential component of the image velocity, which provides the velocity shift to resolve the directional ambiguities, is summarized as:

$$v_t = 2\omega L_2 \qquad \text{for PIV with single rotating mirror} \tag{14a}$$

$$v_t = 2\omega d \sin 2\theta \qquad \text{for PIV with two co-rotating mirrors} \tag{14b}$$

The single-mirrored PIV system generates a constant velocity shift, whereas a two-mirrored system provides a variable velocity shift, depending on the mirror angles at which PIV images are taken. This capability of readily adjusting the amount of velocity shift, without a need of changing the mirror rotational speed ω, is an additional advantage of a two-mirrored system, as the amount of velocity shift must be adjusted based on the measured flow velocity range.

EXPERIMENTAL VERIFICATION

Experiments have been performed using a synthesized image of two-dimensionally distributed 11 × 11 dots of constant intervals that simulate nonmoving particles in flow. Double-exposed photographs were taken at the mirror angles of $\theta = 45° \pm 3°$ (Fig. 6) and $45° \pm 5°$ (Fig. 7) to examine the amount and uniformity of the systematic errors for both single- and double-mirror configurations. The original photographic images have been digitally enhanced, and the dot images have been highlighted with different symbols to distinctively show their counterparts taken at the two different mirror angles in each image. Note that the images were taken at exaggerated mirror angles that readily show the AC and DC components of the dot displacement between the two images.

The velocity shift shown by the DC components of the displacement span approximately one-half dot interval per unit degree of the mirror rotation angle. The AC components of the displacement result from the systematic image errors, and, after subtracting the DC components, the vector displacements of paired dots represent the image biasing. The results for the co-rotating two-mirror configuration (Figs. 6b and 7b) provide uniformly distributed systematic image errors as described by Eq. (13b). However, the systematic errors for the single rotating mirror (Fig. 6a and 7a) are spatially distributed in their magnitudes and directions as shown in Eq. (8) or Eq. (13a). Therefore, the co-rotating two-

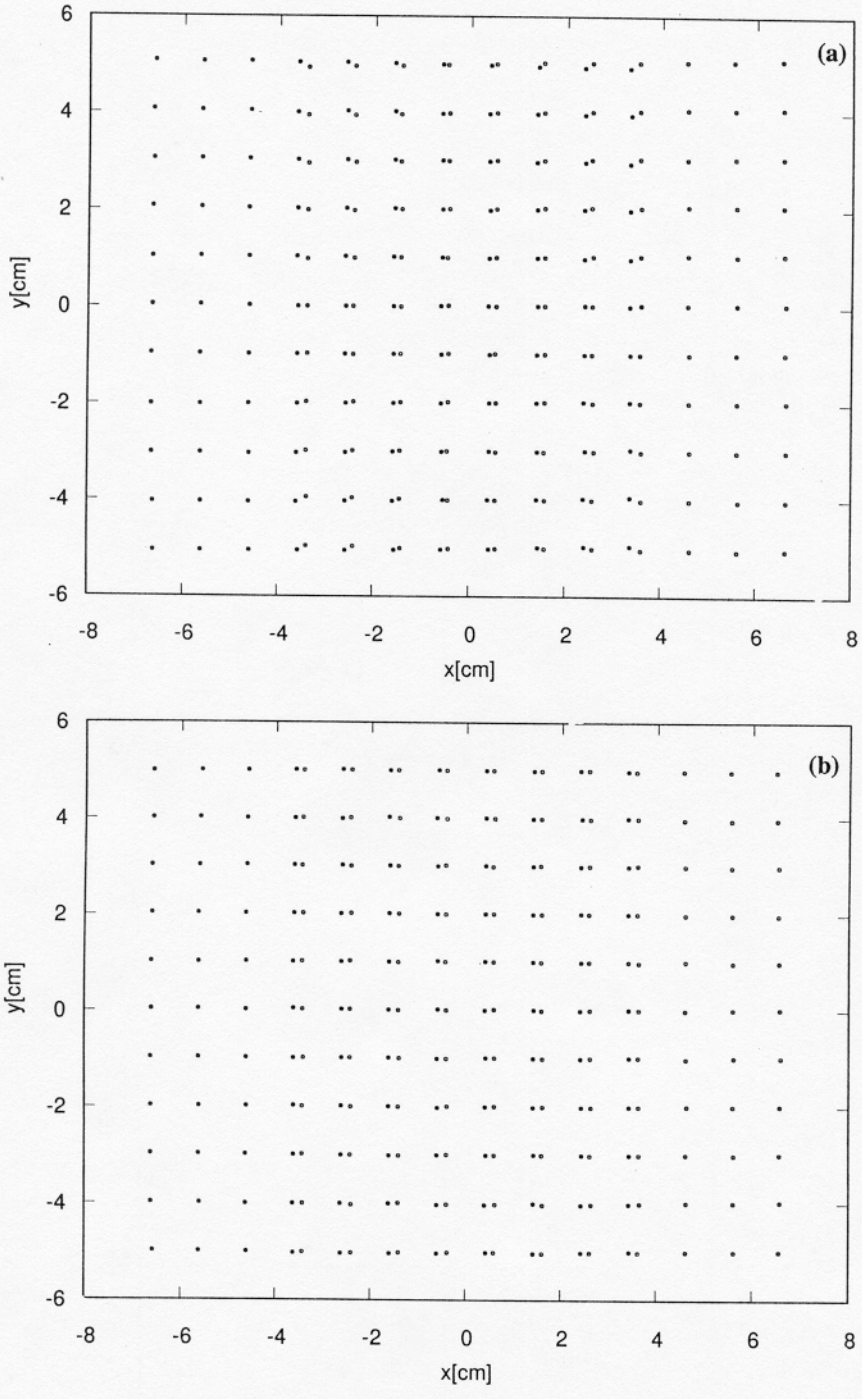

Fig. 6 Digitally enhanced PIV images of synthesized 11 × 11 stationary dots marked by different symbols indicating their recordings at different mirror angles $\theta = 45° - 3°$ and $45° + 3°$: (a) PIV image for a single mirrored system, and (b) PIV image for two co-rotating mirror system.

mirror configuration provides uniform errors that can be readily corrected for the PIV analysis, whereas the conventional single-mirror configuration requires complicated and tedious numerical corrections due to its nonuniformly distributed image biasing.

CONCLUSION

Detailed and comprehensive image kinematics have been developed for the image velocity reflected by a mirror under an arbitrary movement. The developed image kinematics not only identifies the systematic image errors caused by a single rotating mirror PIV system but also fully analyzes the proposed idea of using two co-rotating mirrors. A new configuration with two co-rotating mirrors, instead of one, significantly reduces the systematic errors when the PIV images are taken at mirror slope angles $\theta = 45° \pm \delta$ with $\delta \approx 0$. In addition to the fact that the systematic errors are significantly reduced, their magnitudes and directions are uniform on the entire image plane so that they can be readily corrected, whereas the systematic errors occurring from the single mirror configuration are spatially nonuniform and require elaborate numerical corrections.

REFERENCES

1. R. J. Adrian, Image Shifting Technique to Resolve Directional Ambiguity in Double-Pulsed Velocimetry, *Appl. Optics*, vol. 25, pp. 3855–3858, 1986.
2. M. Oschwald, S. Bechle, and S. Welke, Systematic Errors in PIV by Realizing Velocity Offsets with the Rotating Mirror Method, *Experiments in Fluids*, vol. 18, pp. 329–334, 1995.
3. M. Raffel and J. Kompenhans, Theoretical and Experimental Aspects of Image-Shifting by Means of a Rotating Mirror System for Particle Image Velocimetry, *Measurement Science Technology*, vol. 6, pp. 795–808, 1995.

APPENDIX A: DERIVATION OF THE GENERAL EXPRESSION FOR THE REFLECTED IMAGE VELOCITY VECTOR $\vec{v}_{image}$ (EQ. 5))

Substitution of Eq. (3) into Eq. (4) gives the general expression for the image velocity as

$$\begin{aligned}\vec{v}_{image} &= \frac{d\vec{p}'}{dt} = \frac{d}{dt}\{[R]\cdot(\vec{p}-\vec{r}_m)+\vec{r}_m\}\\ &= \frac{d[R]}{dt}\cdot(\vec{p}-\vec{r}_m)+[R]\cdot\frac{d}{dt}(\vec{p}-\vec{r}_m)+\frac{d\vec{r}_m}{dt}\\ &= \frac{d[R]}{dt}\cdot(\vec{p}-\vec{r}_m)+[R]\cdot\vec{v}+(\vec{v}_m-[R]\cdot\vec{v}_m)\\ &= \frac{d[R]}{dt}\cdot(\vec{p}-\vec{r}_m)+[R]\cdot\vec{v}+2(\vec{v}_m\cdot\vec{n})\vec{n}\end{aligned} \tag{A1}$$

where

$$\begin{aligned}\frac{d[R]}{dt}\cdot\vec{r} &= \frac{d}{dt}(\delta_{ij}-2n_in_j)r_j = \frac{d}{dt}(\delta_{ij}-2n_in_j)R_{jk}R_{kl}r_k\\ &= -2(\Omega_in_j+n_i\Omega_j)R_{jk}r_k' \quad \text{with} \quad \Omega_i \equiv \frac{dn_i}{dt}\end{aligned} \tag{A2}$$

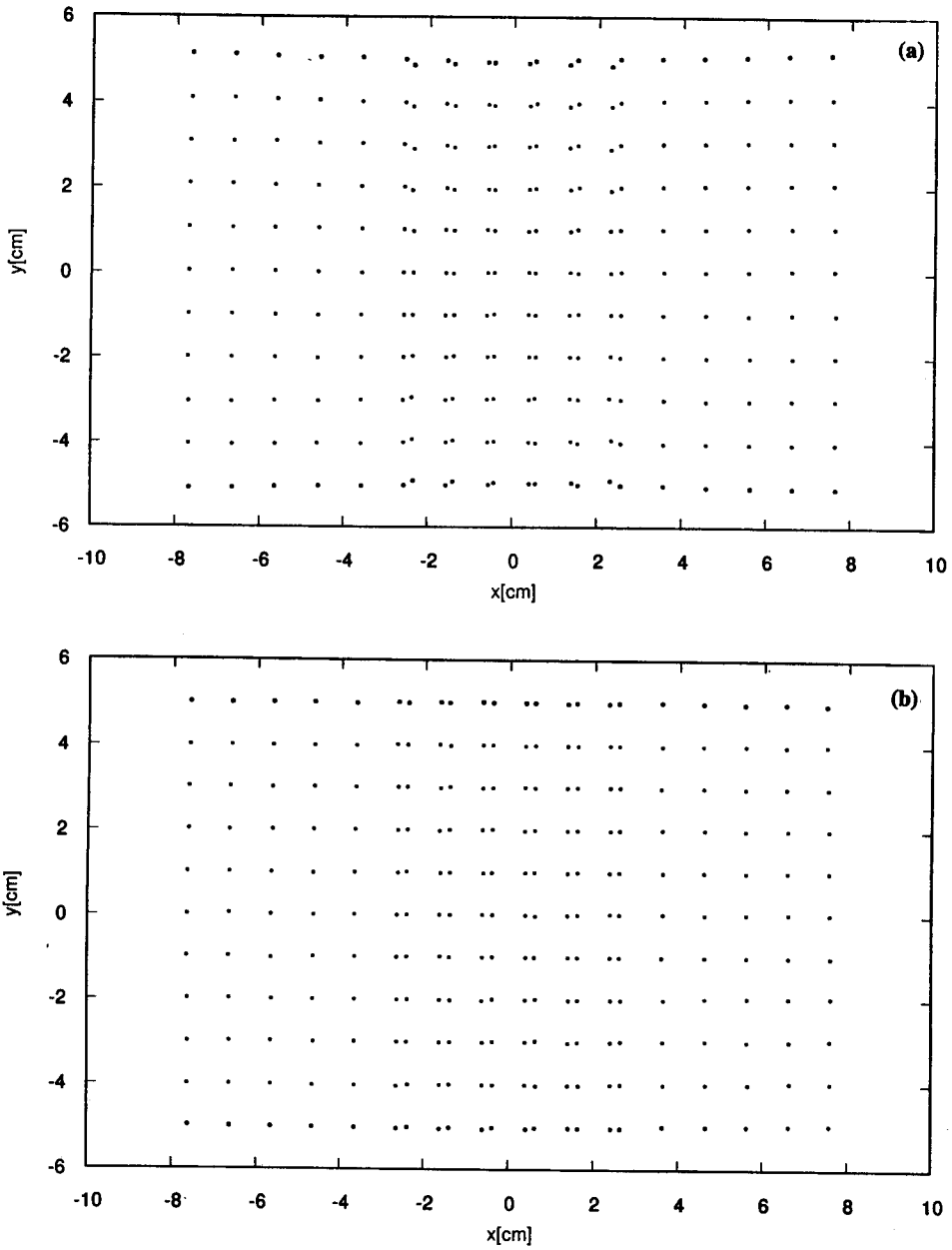

Fig. 7 Digitally enhanced PIV images of synthesized 11 × 11 stationary dots marked by different symbols indicating their recordings at different mirror angles $\theta = 45° - 5°$ and $45° + 5°$: (a) PIV image for a single mirrored system, and (b) PIV image for two co-rotating mirror system.

When the angular velocity of the rotating mirror is defined as $\vec{\omega}$, the amount of the mirror orientation change is given by $\vec{\Omega} = \vec{\omega} \times \vec{n}$. It is noted here that the component parallel to the normal vector does not contribute to the change of orientation. For $\vec{\Omega}$, $\vec{\omega}$ and $\vec{n}$ are mutually perpendicular, and $\vec{n}$ is a unit vector, $\vec{\omega} = \vec{n} \times \vec{\Omega}$, or equivalently, $\omega_i = \varepsilon_{ijk} n_j \Omega_k$ is satisfied.

Thus,
$$\varepsilon_{ilm}\omega_i = \varepsilon_{ilm}\varepsilon_{ijk}n_j\Omega_k = (\delta_{ij}\delta_{mk} - \delta_{ik}\delta_{mj})n_j\Omega_k = n_i\Omega_m - \Omega_i n_m$$
$$(\Omega_i n_j + n_i\Omega_j)R_{jk} = (\Omega_i n_j + n_i\Omega_j)(\delta_{jk} - 2n_j n_k) \tag{A3}$$

$$= \Omega_i n_k + n_i\Omega_k - 2\Omega_i n_k = n_i\Omega_k - \Omega_i n_k = \varepsilon_{lik}\omega_l = -\varepsilon_{ilk}\omega_l \tag{A4}$$

$$\frac{d[R]}{dt} \cdot \vec{r} = 2\varepsilon_{ilk}\omega_l r'_k = 2\vec{\omega} \times \vec{r}' \tag{A5}$$

where $\vec{r}'$ is identical to $[R] \cdot \vec{r}$ as defined in Eq. (A2).

Substituting Eq. (A5) into Eq. (A1) gives the general expression for the image velocity vector of Eq. (5) as:

$$\vec{v}_{image} = 2\vec{\omega} \times \{[R] \cdot (\vec{p} - \vec{r}_m)\} + 2(\vec{v}_m \cdot \vec{n})\vec{n} + [R] \cdot \vec{v} \tag{5}$$